NÖHÜ Müh. Bilim. Derg. / NOHU J. Eng. Sci., 2025; 14(3), 965-973

Niğde Ömer Halisdemir Üniversitesi Mühendislik Bilimleri Dergisi
Niğde Ömer Halisdemir University Journal of Engineering Sciences

Araştırma makalesi / Research article

www.dergipark.org.tr/tr/pub/ngumuh / www.dergipark.org.tr/en/pub/ngumuh

Investigation of genetically-optimized pixel monopole patch antennas for miniaturization and wideband applications

Minyatürleştirme ve geniş bant çalışmaları için genetik olarak optimize edilmiş piksel monopol yama antenlerin incelemesi

Çağatay Aydın[1,*]

Ege Üniversitesi, Elektrik-Elektronik Mühendisliği Bölümü, 35100, İzmir Türkiye

Abstract

A pixel-based synthesis method driven by a genetic algorithm is applied to a rectangular monopole-patch antenna on FR-4. A 7x13 grid with 5 mm x 5 mm pixels is optimized with a single $|S_{11}|$ objective to realize two contrasting designs: a miniaturized antenna that shifts resonance from 3.5 GHz to 1 GHz while reducing the linear size by 65%, and a wideband antenna that maintains $|S_{11}| \leq -10$ dB across 1.9-6 GHz. Full-wave CST simulations validate both cases without altering substrate or feed. The miniaturized version is bandwidth-limited, whereas the wideband version exhibits radiation-pattern variation—shortcomings that stem from the deliberately simple cost function. Results confirm the versatility of pixel antennas and indicate that multi-objective or machine-learning-assisted optimization can further enhance performance.

Keywords: Pixel antenna, Antenna optimization, Genetic algorithm, Miniaturization, Wideband monopole

Öz

Bu çalışmada, FR-4 üzerinde dikdörtgen monopole-yama antene genetik algoritma destekli piksel tabanlı bir tasarım yöntemi uygulanmıştır. 5 mm x 5 mm boyutlu pikseller ile 7x13 olarak pikselleştirilmiş yapı, yalnızca $|S_{11}|$'e bağlı optimize edilerek iki farklı tasarım elde edilmiştir: rezonansı 3.5 GHz'ten 1 GHz'e kaydırarak boyutu doğrusal olarak %65 azaltan minyatür anten ve 1.9-6 GHz aralığında $|S_{11}| \leq -10$ dB sağlayan geniş bant anten. Her iki tasarım da besleme veya substrat değiştirmeden tam dalga CST benzetimleriyle doğrulanmıştır. Basit maliyet fonksiyonuna bağlı olarak mini anten dar bant genişliği, geniş bant anten ise desen değişkenliği göstermektedir. Sonuçlar piksel anten yaklaşımının esnekliğini gösterirken, çoklu hedefli veya makine öğrenmesi destekli optimizasyonlarla performansın daha da iyileştirilebileceği görülebilir.

Anahtar kelimeler: Piksel anten, Anten optimizasyonu, Genetik algoritma, Minyatürizasyon, Geniş bant monopol

1 Introduction

The continuous advance of wireless communication systems demands antenna solutions that are both compact and capable of operating over wide or multiple frequency bands [1], [2]. Seamless integration into devices such as mobile terminals and IoT sensors, wearable electronics face the challenge of miniaturization [3], [4]. At the same time, support for diverse standards such as 5G, WLAN and Bluetooth requires antennas with broad or reconfigurable frequency coverage [2], [5]. Although planar monopole antennas are inherently low profile and can offer appreciable bandwidth [6], achieving simultaneous wideband performance and pronounced size reduction remains difficult [1], [4].

Conventional miniaturization techniques, for example loading the radiator with high-permittivity substrates or introducing meanders, slots and defected-ground structures (DGS) [2], [6], [7], seek to lengthen the electrical path within a restricted physical volume. Classical wideband strategies, in turn, reshape the antenna element and ground plane or employ specialized feeding arrangements [1]. While successful, these approaches often involve design trade-offs and may lack the flexibility needed to satisfy multifunctional requirements.

Pixel antennas offer a highly adaptable alternative. In this concept the radiating surface is discretized into an array of "pixels", each of which may be metallic or non-metallic (or switch-controlled) [8-10]. By selecting the pixel states, the effective geometry and current distribution can be reshaped in order to tailor resonant frequency, bandwidth, radiation pattern or polarization [8], [11–14].

This versatility is particularly advantageous for miniaturization: optimization algorithms can identify pixel configurations that lower the fundamental resonance without enlarging the footprint. Using a 10x10 pixel grid, Lamsalli et al. [10] achieved an 82% size reduction, shifting the resonance from 4.9 GHz to 2.16 GHz. The same principle can be exploited to obtain wideband behavior, as optimized pixel arrangements are able to excite multiple resonant modes and create complex current paths [14], [15]. For instance, in [14], a low-profile pixel antenna with more than 40% bandwidth in the L-band is reported, while stacked pixelated layers have been proposed for dual-band IoT applications [5].

* Sorumlu yazar / Corresponding author, e-posta / e-mail: cagatay.aydin@ege.edu.tr (Ç. Aydın)
Geliş / Received: 19.04.2025 Kabul / Accepted: 14.05.2025 Yayımlanma / Published: 15.07.2025
doi: 10.28948/ngumuh.1679692

Because the number of possible pixel combinations grows exponentially with grid size, computational optimization is indispensable [15], [16]. Evolutionary algorithms (EAs) are widely adopted [17]: genetic algorithms (GAs) have been used for frequency reconfiguration, pattern steering and miniaturization [10], [11], [18], and binary particle-swarm optimization (BPSO) has been adapted to the discrete pixel topology [5]. More advanced techniques include successive Boolean optimization (SEBO) [11], N-port characteristic-mode-analysis-driven searches [15], adjoint-method optimizers such as the Method of Moving Asymptotes (MMA) [9], and machine-learning-assisted schemes based on convolutional or reinforcement-learning models [13], [19]-[21].

This paper demonstrates the application and versatility of the pixel antenna approach using a systematic design methodology to enhance monopole antenna performance. The work aims for two distinct design objectives using the same initial rectangular monopole patch geometry and fundamental $|S_{11}|$-based cost function: the first being substantial miniaturization for operation near 1 GHz and the second being wideband operation covering 2–6 GHz. The pixel configurations are optimized using a GA, selected for its demonstrated effectiveness in miniaturization tasks [10]. Full-wave electromagnetic simulations are employed to evaluate the resulting antenna geometries. The results presented illustrate that this consistent methodology can successfully yield designs addressing both miniaturization and wideband impedance matching requirements, albeit with performance limitations (such as bandwidth restriction in the miniaturized case and pattern instability in the wideband case) directly attributable to the simplicity of the chosen cost function. This underscores the flexibility of the pixel approach and highlights the critical role of the objective function in achieving fully optimized, application-specific performance.

2 A systematic methodology for pixel-based antenna design and optimization

In this section, two examples will be shown for miniaturization application and wideband application by utilizing pixel antenna approach. But before these examples, the design procedure should be explained.

2.1 Initial monopole geometry and dimensional analysis

A rectangular monopole patch antenna was selected to implement the pixel antenna approach for simplicity. The 0.7-6 GHz frequency range was chosen because it covers many widely used wireless applications, including GSM 1, GSM 2, 3G, LTE, 5G, Wi-Fi, Wi-Max and Bluetooth. The rectangular monopole patch antenna was designed on loss free FR4 ($\varepsilon_r = 4.3$, thickness 1.6 mm) due to its low cost. For the simulations, the FR4 was initially modeled as lossless to focus on the geometric optimization effects.

In the first step, 3.5 GHz was chosen as the center frequency for the rectangular patch antenna, as it approximately represents the arithmetic mean of the target frequency range. The equations needed to determine the dimensions of the rectangular patch antenna are available in the literature [22], [23]. The calculated width and length were 26 mm x 20 mm, respectively, for the specified center frequency.

In the following step, the rectangular patch antenna was transformed into a monopole structure to achieve a wide frequency range. For this purpose, the ground plane was designed to be 3 mm shorter than the feed line. Therefore, the dimensions for the reference antenna are provided in Table 1, and the antenna geometry along with its simulation results are presented in Figure 1 and Figure 2, respectively. The substrate dimensions were chosen to be 70 mm x 70 mm (WSUB x LSUB). The initial antenna was simulated using CST MWS.

Tablo 1. Dimensions of the initial rectangular monopole patch antenna ($in\ mm$)

WA	LA	WF	LF	WGND	LGND
26	20	1.5	31	70	28

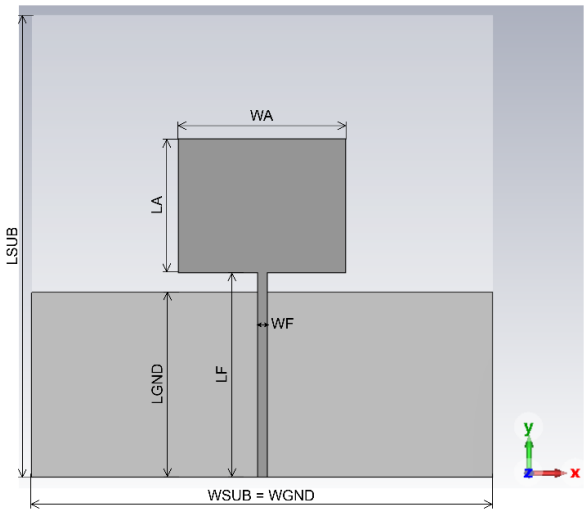

Figure 1. Geometry of initial rectangular monopole patch antenna

At this stage, the procedure requires finalizing the antenna dimensions for both miniaturization process and wideband performance which should be achieved separately, as previously discussed. As illustrated in Figure 2(a), the initial design already supports wide frequency operation; however, achieving lower frequencies in the target range becomes challenging under realistic miniaturization constraints. For example, designing a patch antenna at 1 GHz would necessitate dimensions of approximately 90 mm x 90 mm. Therefore, more moderate dimensions should be selected to simplify the optimization process and cover the 0.7-1 GHz band. Consequently, the width of 65 mm and the length of 35 mm were chosen for the final antenna, while the other parameters specified in Table 1 remain unchanged as depicted in Figure 3.

Since the final design has already been established, the next step is to apply the pixel approach by utilizing an appropriate optimization procedure. The details of this process will be discussed in the following section.

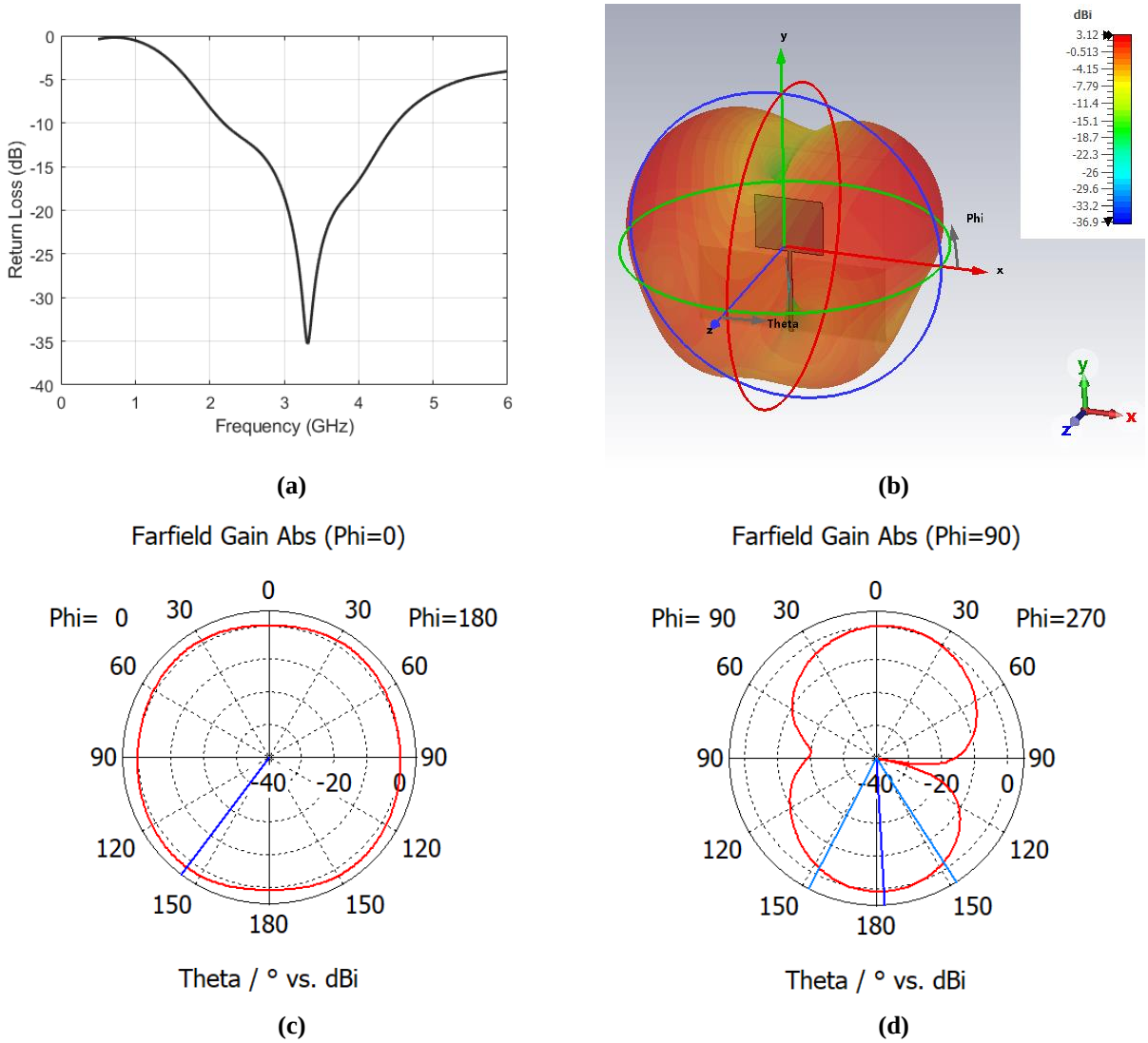

(a) **(b)** **(c)** **(d)**

Figure 2. Simulation results of initial rectangular monopole patch antenna: **(a)** Return loss (dB), **(b)** 3D polar plot (Gain) at 3.5 GHz, **(c)** Radiation pattern (E-Plane) at 3.5 GHz., **(d)** Radiation pattern (H-plane) at 3.5 GHz.

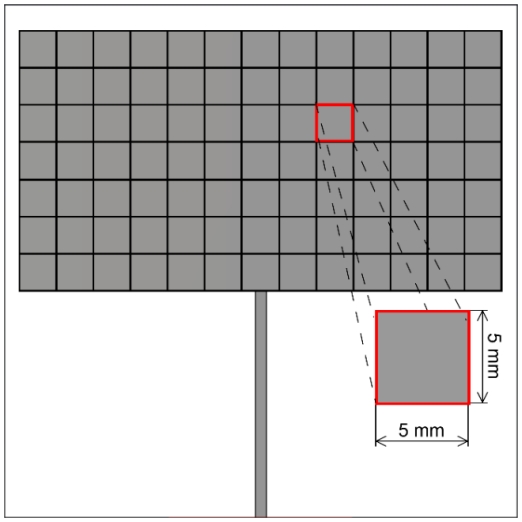

Figure 3. Pixelated geometry of final rectangular monopole patch antenna with $65mm \times 35mm$ dimension

2.2 Optimization procedure utilizing the pixel approach

In the introduction, we briefly noted that many studies employ standard optimization methods such as GA, particle swarm optimization (PSO), and differential evolution (DE in addition to developing novel, more efficient algorithms. However, the primary objective of this manuscript is to investigate the versatility of pixel antennas for a range of applications. Therefore, one of the most widely used optimization methods, the GA, was selected for this work.

Although CST was used to verify the designed antennas, the GA optimization routine with default settings was executed in MATLAB, a common practice for such applications. A brief outline of this routine is provided below with the corresponding flowchart is depicted in Figure 4:

- A pixel value of "1" indicates metal presence, while "0" indicates the absence of metal.
- The antenna geometry is divided into pixels, forming a matrix of "1"s and "0"s.

- This matrix is used to generate the antenna geometry, which is then exported to CST.
- CST simulates the antenna geometry and returns the results to MATLAB.
- A cost value is calculated in MATLAB based on specified parameters and the target frequency range.
- New generations are created, and these steps are repeated until the optimization routine terminates.

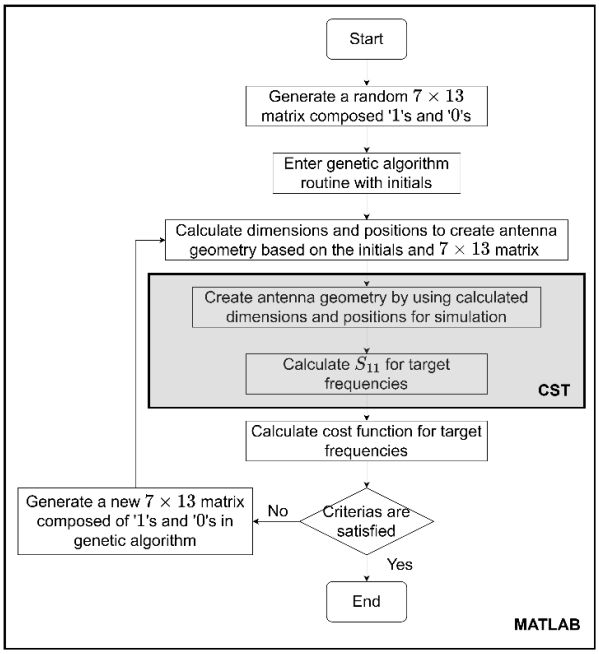

Figure 4. Flowchart of optimization routine involving MATLAB and CST interaction.

In this study, each pixel measures 5 mm x 5 mm, corresponding to a 7x13 matrix with a total of 91 pixels. At the maximum target frequency of 6 GHz, this dimension is approximately $\lambda/10$, which can be considered a moderate size. Larger pixel dimensions might reduce the likelihood of meeting the desired cost criteria or significantly increase computation time. The suitability of this pixel size will be discussed in the following section.

Reference [10], proposes the following cost function,

$$cost = \left| \frac{1}{N} \sum_{i=1}^{N} Q(f_i) \right| \tag{1}$$

where,

$$Q(f_i) = \begin{cases} |S_{11}(f_i)|, & for\ S_{11} \geq -10\ dB \\ +10\ dB, & for\ S_{11} \leq -10\ dB \end{cases}$$

Equation (1) is a fundamental equation used to calculate the cost function. In this equation, f_i is denoting the target frequencies and N is the total number of target frequencies. The reason for choosing this equation is to demonstrate that pixel antennas can be adapted to a variety of applications with minimal effort, as previously mentioned. It is also evident that a more complex or tailored cost function for a specific application could facilitate reaching the desired goals more efficiently.

It should be noted that the effect of a pixelated ground plane was intentionally excluded from this study. Although such structures such as defected ground structures [2] are known to improve size reduction or bandwidth performance, including them would require more complex analysis. This could shift the focus of the study toward additional parameters such as coupling, which are beyond the intended scope for this manuscript.

This section introduced the fundamental aspects of the proposed methodology. The pixel-based approach for defining the antenna geometry, allowing for a diverse range of configurations, was presented. The GA-based optimization framework was also described, highlighting the integration between MATLAB for cost function calculation and CST Microwave Studio for electromagnetic analysis and final performance verification. The next section presents examples of this methodology and discusses their results.

3 Simulation results and discussion

In order to demonstrate the versatility inherent in the pixel antenna approach, two primary design objectives as mentioned earlier will be covered: miniaturization and wideband operation. Both optimization scenarios utilize the identical baseline antenna geometry, pixel count, and pixel size (Figure 3), as well as the same cost function (Equation (1)). The simulation results obtained for each case will be presented and discussed in the context of these constraints, evaluating the extent to which the target performance values were achieved.

3.1 Case I: Miniaturization

The miniaturization objective targeted the 0.7-1 GHz frequency range. For context, conventional rectangular patch antennas operating at these frequencies would require significant physical dimensions (approximately 130 mm x 100 mm at 0.7 GHz and 90 mm x 70 mm at 1 GHz). In contrast, our approach applied GA-based optimization to the predefined pixelated structure described previously. Figure 5 presents the simulated return loss characteristics for three of the best-performing pixel configurations obtained by the GA optimization. The simulation results show that while satisfactory operation was achieved near the upper edge of the band (around 1 GHz), the performance requirement was not met across the entire target range. Potential factors contributing to this limitation may include the size of the pixels or the simplicity of the cost function (Equation (1)) used for this application. It is acknowledged that achieving broadband impedance matching in electrically small antennas is inherently challenging due to Chu limit [23]; advanced optimization strategies incorporating machine learning techniques [13], [18], [19] or more complex, tailored cost functions are actively researched areas that could potentially enhance performance for such demanding requirements.

Figure 6 depicts the geometries resulting from three of the best-performing configurations obtained from the GA-based optimization. Inspection of these pixel arrangements

indicates that the optimization algorithm tends to form structures that effectively increase the electrical path length of the surface currents. This strategy is consistent with achieving resonance at lower target frequencies within the fixed antenna footprint. In addition, Figure 6 also presents the simulated radiation patterns for these designs at 1 GHz.

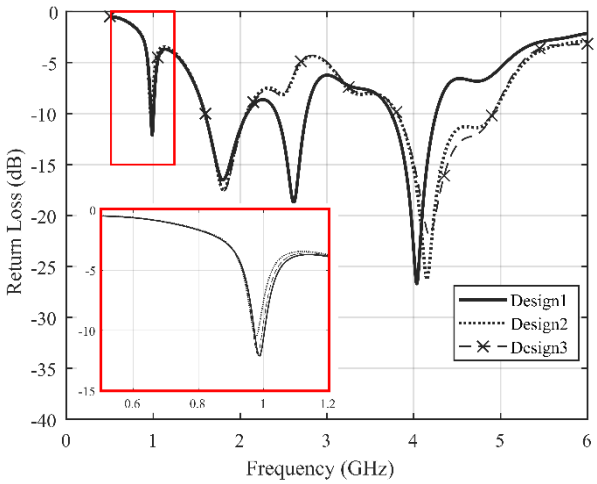

Figure 5. Return loss (dB) plot of three of best designs for Case I.

Due to the overall similarity in the optimized geometries, the radiation patterns exhibit no differences. The simulated maximum gain for these configurations is approximately 1.8 dBi. Furthermore, the figure includes the surface current distributions, visualized using a 0-100 A/m linear scale. While slight variations in maximum of current magnitude exist between the designs, the overall distribution consistently highlights the dominant current paths established by the pixel optimization.

Regarding the radiation patterns, it is observed that for these GA-optimized miniaturized designs (Figure 6), the Phi=90° plane tends to exhibit the most omnidirectional-like characteristic. For the initial rectangular monopole patch antenna, its H-plane (Figure 2(d), Phi=90°) displays the expected broadly omnidirectional behavior, while the E-plane (Figure 2(c), Phi=0°), especially with a limited display scale in its original presentation, can appear more directional, as is typical for monopoles in that principal plane. The differences in radiation pattern characteristics, including the apparent orientation of the most omnidirectional plane for the miniaturized antennas, are a direct consequence of the pixel-based optimization. The GA modifies the antenna geometry to achieve miniaturization by creating complex current paths, which fundamentally alters the radiation mechanism compared to the simpler initial structure.

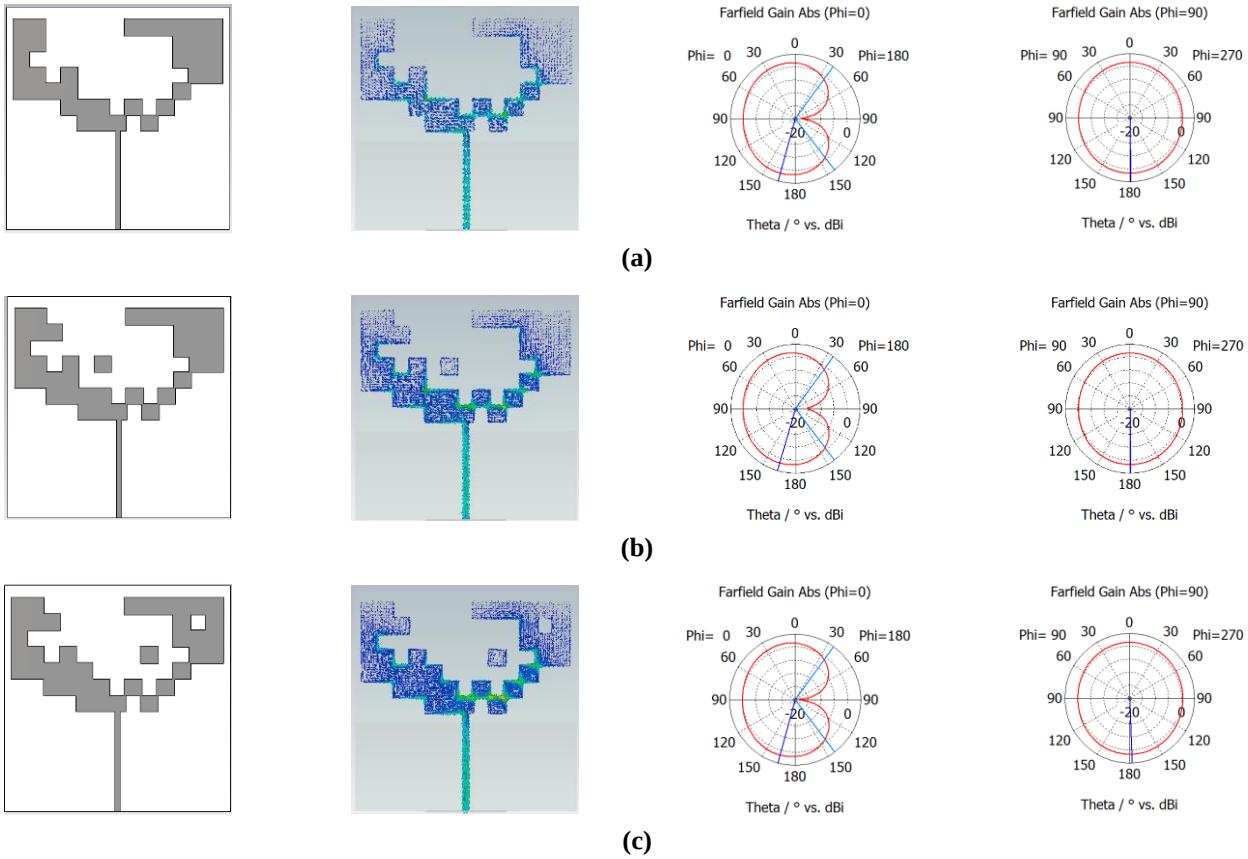

Figure 6. Antenna geometries and corresponding distribution of surface current plots and radiation patterns (E- and H-Plane), respectively at 1 GHz obtained by GA-based optimization for Case I: **(a)** Design1, **(b)** Design2, **(c)** Design3

3.2 *Case II: Wideband operation*

Addressing the second objective, wideband operation, the target frequency range was set from 07.-5.8 GHz. To emphasize the versatility of the pixel approach, the same initial geometry, constraints, and cost function (Equation (1)) utilized for miniaturization were applied here. Figure 7 depicts the simulated return loss results, comparing the initial rectangular monopole antenna with three optimized pixel configurations obtained via GA-based optimization. This comparison clearly shows the significant bandwidth expansion that was achieved. Especially, Design3 exhibits the most promising wideband characteristics, covering the 1.9 GHz to 6 GHz range (and potentially beyond), although it does not meet the matching requirement below 1.9 GHz within the target range. As with the miniaturization case, this limitation might be due to the same factors such as pixel size or the specific cost function employed. Nonetheless, the achieved bandwidth for Design3 indicates considerable potential, suggesting that further improvements are possible with more advanced optimization strategies or refined cost functions.

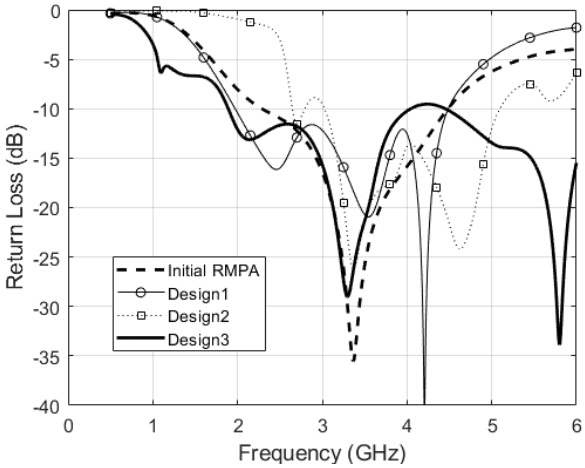

Figure 7. Return loss (dB) plots of antennas designed for Case II.

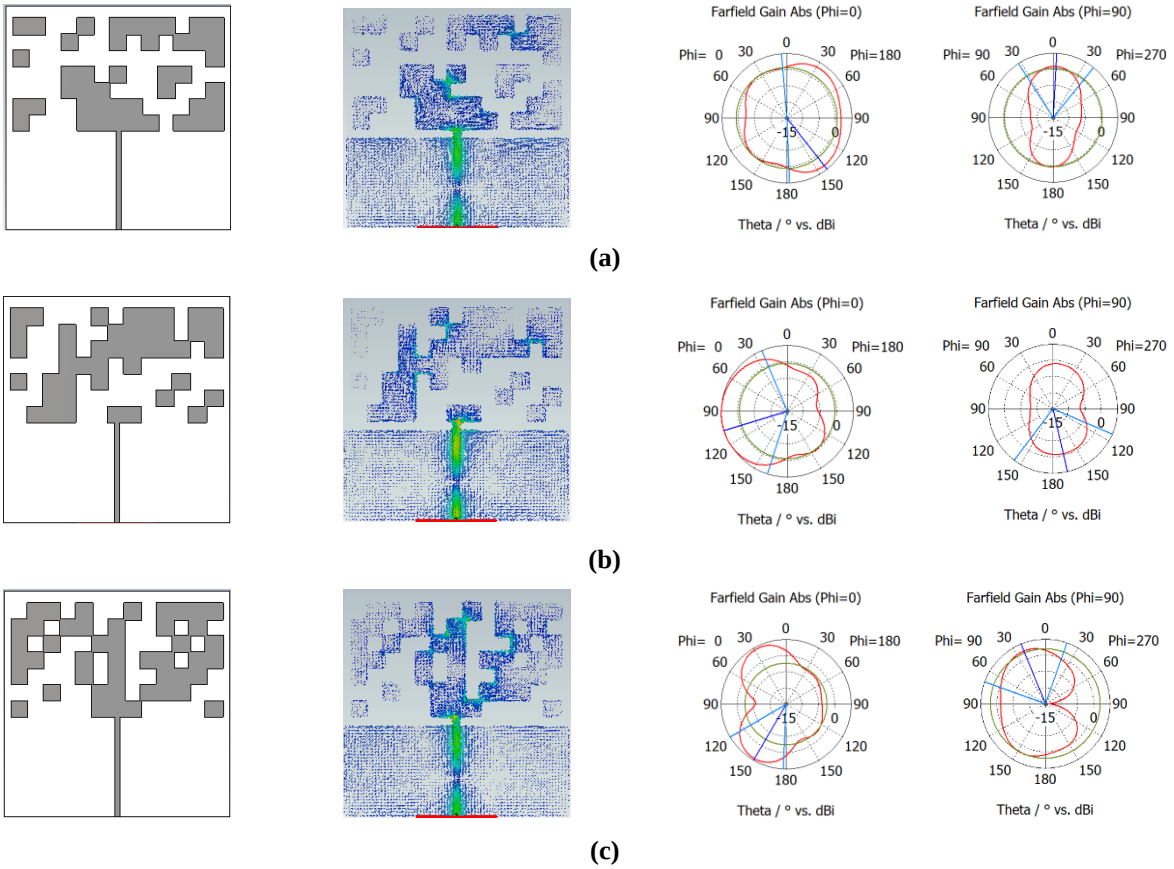

Figure 8. Antenna geometries and corresponding distribution of surface current plots and radiation patterns (E- and H-Plane), respectively at 3.5 GHz obtained by GA-based optimization for Case II: **(a)** Design1, **(b)** Design2, **(c)** Design3.

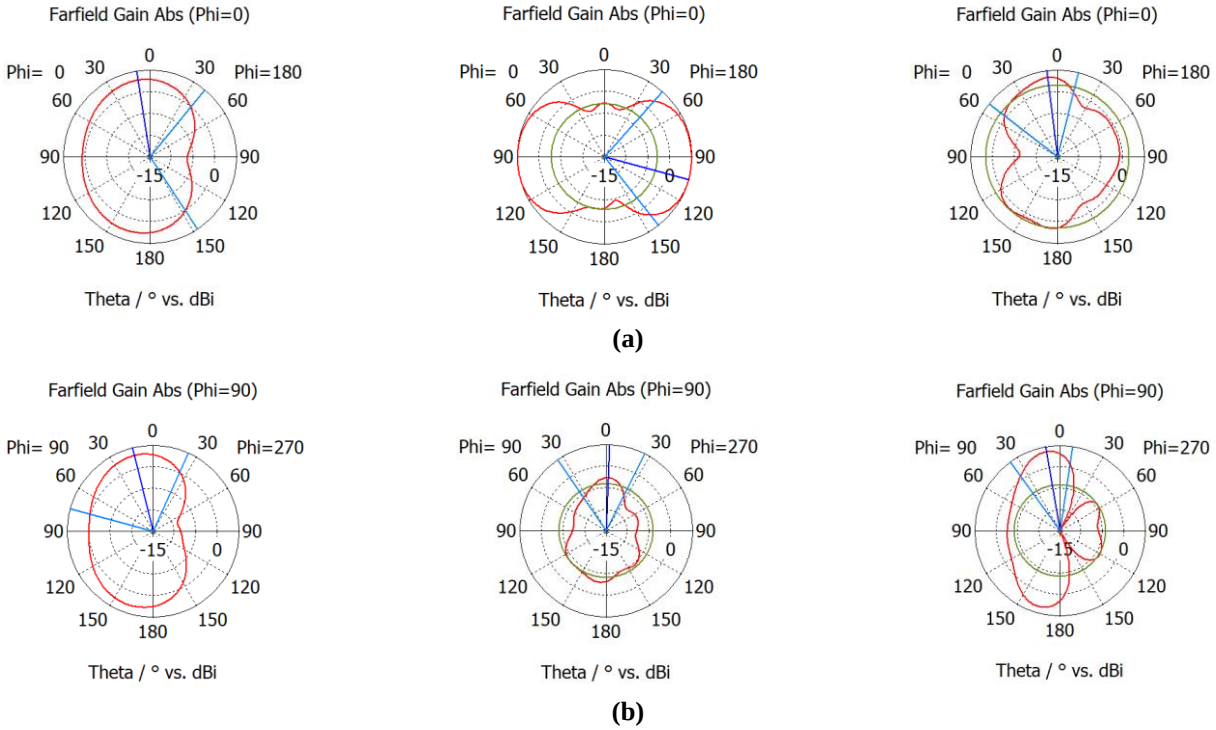

Figure 9. Radiation patterns of Design3 antenna at 2.5 GHz, 4.5 GHz and 5.5 GHz, respectively: **(a)** E-Plane, **(b)** H-Plane.

Figure 8 depicts the geometries for antennas Design1, Design2, and Design3 with their respective radiation patterns simulated at 3.5 GHz. These three designs were specifically chosen from the optimization results meeting the return loss requirement to demonstrate the geometric variety achievable with the pixel approach. As can be seen, although satisfying the primary frequency target, their optimized pixel structures differ considerably. Consequently, each antenna exhibits a distinct radiation pattern due to its unique geometry. This clearly shows the strong relationship between the antenna's structure and its radiation characteristics. It highlights that optimizing solely for target return loss does not guarantee a specific radiation pattern, and incorporating pattern metrics into the cost function would be necessary for many practical applications [6]. For the presented wideband designs, the simulated maximum gain is approximately 5 dBi for each one. The corresponding surface current distributions are also visualized in Figure 8, using a consistent linear scale of 0-40 A/m, further illustrating the different current paths associated with each unique geometry.

An essential characteristic of wideband antennas, beyond expected return loss, is the stability of their radiation patterns across the operational frequency range. Figure 8(c) presents the radiation pattern for Design3 at 3.5 GHz, while Figure 9 illustrates the patterns at additional frequencies such as 2.5 GHz, 4.5 GHz, and 5.5 GHz within its operational band. Comparison across these frequencies reveals significant variations in the radiation pattern's shape and directivity. This indicates that, despite achieving wideband operation (as shown in Figure 7), Design3 lacks the pattern stability often required for practical wideband applications. Such an outcome is directly attributable to the cost function employed (Equation (1)), which solely targeted the minimization of the return loss. Achieving consistent radiation patterns necessitates the inclusion of appropriate pattern stability metrics within the optimization objective function.

4 Conclusion

A single pixel-antenna framework, combined with a GA optimizer, has produced two distinct monopole-patch designs from an identical 7x13 grid: a 65 mm x 35 mm antenna resonating at 1 GHz with almost greater than 65% size reduction, and a wideband variant covering 1.9-6 GHz (≈ 80% fractional bandwidth). These outcomes confirm that pixelation can address divergent specifications such as miniaturization and broadband matching without modifying substrate, feed, or manufacturing process.

The exclusive reliance on a $|S_{11}|$ cost function simplifies implementation but imposes clear limits: reduced bandwidth and gain (1.8 dBi) in the compact case and radiation-pattern instability below 2 GHz in the wideband case. Future studies will therefore adopt multi-objective criteria that include radiation efficiency, pattern stability and, for electrically small antennas, Chu-constrained bandwidth. The effect of a pixelated ground plane will also be investigated, as it may offer additional bandwidth enhancement or size reduction while introducing new design trade-offs. Machine-learning-accelerated surrogate models will also be explored to cut optimization time. Finally, physical prototyping and low-frequency extensions (< 800 MHz) will be studied to demonstrate further size reduction and to validate the simulated results experimentally.

Conflict of interest

The author declares that there is no conflict of interest.

Similarity (iThenticate): 4%

References

[1] M. A. Ullah, R. Keshavarz, M. Abolhasan, J. Lipman, and N. Shariati, Multiservice compact pixelated stacked antenna with different pixel shapes for IoT applications, IEEE Internet Things Journals, vol. 10, no. 22, pp. 19883–19897, 2023. https://doi.org/10.1109/JIOT.2023.3281816

[2] M. C. Derbal, M. F. Nakmouche, M. Nedil, A. Amma, D. E. Fawzy and M. F. A. Sree, Dual-band antenna design using pixeled DGS for energy-harvesting applications, 9th International Conference on Electrical and Electronics Engineering (ICEEE), pp. 147–150 Antalya, Türkiye, 29-31 Mar. 2022. https://doi.org/10.1109/ICEEE55327.2022.9772605

[3] D. Mair and D. Baumgarten, Evolutionary optimisation of pixelated IFA-inspired antennas, Science Reports, vol. 14, no. 1, Art. no. 26664, Nov. 2024. https://doi.org/10.1038/s41598-024-77695-x

[4] M. Shubbar and B. Rakos, A self-adapting, pixelized planar antenna design for infrared frequencies, Sensors, vol. 22, no. 10, p. 3680, May 2022. https://doi.org/10.3390/s22103680

[5] A C. Suresh, T. S. Reddy, B. T. P. Madhav, S. Alshantri, W. El-Shafai, S. Das and V. Sorathiya, A novel design of spike-shaped miniaturized 4x4 MIMO antenna for wireless UWB network applications using characteristic mode analysis, Micromachines, vol. 14, no. 3, p. 612, Jan. 2023. https://doi.org/10.3390/mi14030612

[6] D. Rodrigo, B. A. Cetiner, and L. Jofre, Frequency, radiation-pattern and polarization-reconfigurable antenna using a parasitic pixel layer, IEEE Transactions on Antennas and Propagation, vol. 62, no. 6, pp. 3422–3427, Jun. 2014. https://doi.org/10.1109/TAP.2014.2314464

[7] J. Jayasinghe, J. Anguera, and D. Uduwawala, On the behavior of several fitness functions for genetically optimized microstrip antennas, International Journal of Scientific World, vol. 3, no. 1, pp. 53–58, Feb. 2015. https://doi.org/10.14419/ijsw.v3i1.4132

[8] T. Qiao, F. Jiang, S. Shen, Z. Zhang, M. Li and C. Y. Chiu, Pixel-antenna optimization using the adjoint method and the method of moving asymptotes, IEEE Transactions on Antennas and Propagation, vol. 71, no. 3, pp. 2873–2878, Mar. 2023. https://doi.org/10.1109/TAP.2023.3240563

[9] S. Song and R. D. Murch, An efficient approach for optimizing frequency-reconfigurable pixel antennas using genetic algorithms, IEEE Transactions on Antennas and Propagation, vol. 62, no. 2, pp. 609–620, Dec. 2013. https://doi.org/10.1109/TAP.2013.2293509

[10] M. Lamsalli, A. El Hamichi, M. Boussouis, N. A. Touhami, and T. Elhamadi, Genetic-algorithm optimization for microstrip patch antenna miniaturization, Progress in Electromagnetics Research Letters, vol. 60, pp.113–120, 2016. https://doi.org/10.2528/PIERL16041907

[11] S. Shen, Y. Sun, S. Song, D. P. Palomar, and R. D. Murch, Successive Boolean optimization of planar pixel antennas, IEEE Transactions on Antennas and Propagation, vol. 65, no. 2, pp. 920–925, Feb. 2017. https://doi.org/10.1109/TAP.2016.2634399

[12] F. Jiang, S. Shen, C.-Y. Chiu, Z. Zhang, Y. Zhang, and Q. S. Cheng, Pixel-antenna optimization based on perturbation-sensitivity analysis, IEEE Transactions on Antennas and Propagation, vol. 70, no. 1, pp. 472–486, July. 2021. https://doi.org/10.1109/TAP.2021.3097104

[13] Q. Wu, W. Chen, C. Yu, H. Wang, and W. Hong, Machine-learning-assisted optimization for antenna-geometry design, IEEE Transactions on Antennas and Propagation, vol. 72, no. 3, pp. 2083–2095, Jan. 2024. https://doi.org/10.1109/TAP.2023.3346493

[14] M. Rammal, M. Majed, E. Arnaud, J. Andrieu, and B. Jecko, Small-size wide-band low-profile “pixel antenna”: Comparison of theoretical and experimental results in L-band, International Journal of Antennas and Propagation, vol. 2019, no. 1, 2019. https://doi.org/10.1155/2019/3653270

[15] F. Jiang, C.-Y. Chiu, S. Shen, Q. S. Cheng, and R. Murch, Pixel-antenna optimization using N-port characteristic-mode analysis IEEE Transactions on Antennas and Propagation, vol. 68, no. 5, pp. 3336–3347, Jan. 2020. https://doi.org/10.1109/TAP.2019.2963588

[16] J. W. Jayasinghe, Application of genetic algorithm for binary optimization of microstrip antennas: A review, AIMS Electronics and Electrical Engineering, vol. 5, no. 4, pp. 315-333, 2021. https://doi.org/10.3934/electreng.2021016

[17] S. K. Goudos, Optimization of antenna design problems using binary differential evolution, in Handbook of Research on Emergent Applications of Optimization Algorithms, Business Science Reference, IGI Global, pp. 614-636, Jan. 2018. https://doi.org/10.4018/978-1-5225-2990-3.ch026

[18] H. Chen, Z. Wu, S. Li, X. Li, and Q. Liu, Proximal policy optimization reinforcement learning assisted patch antenna design, in Proc. IEEE 12th Asia-Pacific Conference on Antennas and Propagation (APCAP), Bali, Indonesia, 22-25 Jul. 2024. https://doi.org/10.1109/APCAP2011.2024.10881019

[19] Q. Wang, Z. Pang, D. Gao, P. Liu, X. Pang and X. Yin, Machine-learning-assisted quasi-bisection method for pixelated patch-antenna bandwidth optimization, IEEE Antennas Wireless Propagation Letters, vol. 23, no. 12, pp. 4807–4811, Dec. 2024. https://doi.org/10.1109/LAWP.2024.3475628

[20] S. Goudos, Antenna design using binary differential evolution: Application to discrete-valued design problems, IEEE Antennas and Propagation Magazine, vol. 59, no. 1, pp. 74–93, Feb. 2017. https://doi.org/10.1109/MAP.2016.2630041

[21] C. A. Balanis, Antenna Theory: Analysis and Design 3rd ed., New York, USA: Wiley, 2005.
[22] W. L. Stutzman and G. A. Thiele, Antenna Theory and Design, 3rd ed., Wiley, 2012.
[23] L. J. Chu, Physical limitations of omni-directional antennas, Journal of Applied Physics, vol. 19, pp. 1163–1175, 1948. https://doi.org/10.1063/1.1715038